# Small-Signal Modeling and Analysis of an Isolated Bidirectional Battery Charger

Edivan Laercio Carvalho, Emerson Carati, Jean Patric da Costa, Carlos Marcelo de Oliveira Stein, Rafael Cardoso

Federal University of Technology - Paraná - UTFPR, Pato Branco - PR, Brazil
Post-Graduation Program in Electrical Engineering – PPGEE
Static Power Converters Engineering Research Group - ECEE
E-mails: edivan.labensaios@gepoc.ufsm.br, emerson@utfpr.edu.br, jpcosta@utfpr.edu.br, cmstein@utfpr.edu.br, rcardoso@utfpr.edu.br

***Abstract* — This paper presents the small-signal modeling and analysis of an isolated bidirectional DC-DC converter. The converter is implement based on two Full-Bridge converters. The system is designed to act as a charge/discharge controller for battery banks. The model for each mode of operation is developed using the average state-space model approach. To verify the models, simulations are performed using PSIM software in addition to experimental results obtained from a 200 W prototype that connects a 60 V battery bank to a 230 V DC link.**

***Key-Words:*** **Dynamic Models, Small-Signal Analysis, Bidirectional Converters, Charge/Discharge Controller.**

## I. INTRODUCTION

In many systems that use energy storage on batteries - like power generation systems, electric vehicles and UPS's (Uninterrupted Power Supply's) – the control of power flow between a primary source and battery banks is required [1], [2]. In these applications, the processes of charge and discharge of the batteries depend on the performance of voltage converters, whose main objective is to adequate the levels of voltages between battery banks (low voltage) and DC links (high voltage). The use of converters is also justified due to the necessity to control the charging current and DC link voltage [3]-[5].

In applications such as energy storage systems, the power management can be realized using unidirectional DC-DC converters. On this approach, different converters make the charge and discharge of the batteries. Therefore, two converters are used in this approach. However, the development of bidirectional converters is interesting to unify the power flow control between a DC link and batteries using a single device. This characteristic is appropriated to improve management energy in generation power systems and to reduce the number of structures involved in those systems [6]-[8].

The application of bidirectional converters in energy storage systems is indicated in many works like [7], [8], [9] and [10]. In those papers, advances related to bidirectional configurations, operation and analysis of such converters on steady state are presented. However, to achieve adequate operation of these systems it is necessary the implementation of a control system to control the charge and discharge of the battery bank.

It is well known that the design of a control system depends on a previous knowledge of the behavior of the plant to be controlled. Hence, it is important to perform an adequate analysis of the transient response of the bidirectional converter considering the battery bank.

To design an adequate control system, some knowledge about the plant is necessary. Considering the bidirectional converter presented in [10] and depicted in Figure 1, this paper presents its modeling considering both operation modes, i. e., charge and discharge.

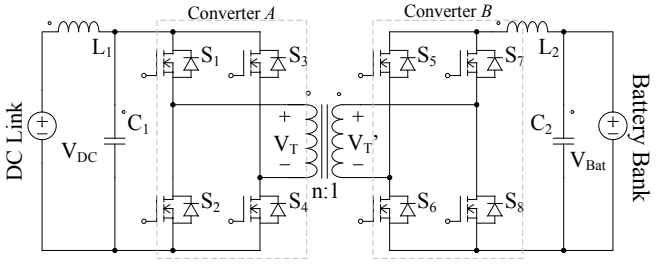


Fig.1. Proposed circuit.

This paper adopts modeling based on the average state-space model. This approach is found on [11], [12] and [13] that describes the use of average models in bidirectional converters. However, these papers disregard the presence of batteries or consider only discharge operation.

This work differs from previous papers by including on the analysis the presence of batteries in both operation modes. It also presents experimental results to validate the proposed models. Many researches found in literature focus on advances in topologies and considers only steady state analysis. Therefore, this paper presents a continuation of [10], which deals only with a steady-state analysis. In this sense, the obtainment and validation of the bidirectional converter models are the main contribution of this work.

Pursuing the aforementioned objectives, this work is organized as follows: in section II, the converter operation is described with the objective to represent the systems using the average state space model. In section III, the small-signal models are obtained and in section IV the validation of the model is presented. Finally, section V concludes the paper.

## II. CONVERTER OPERATION AND MODELLING

According to the circuit depicted in Figure 1, initially, to guarantee the DC link regulation, it is proposed that the inverter on the battery side operates like a current-fed converter (boost converter) during the discharge mode of

operation. During the charge process, the inverter on the DC link side operates like a voltage-fed. Hence, the voltage of DC link can be reduced in the transformer terminals during the charge and, while in discharge, the voltage of batteries can be raised. This operation increases the operational range of the converter voltage gain and maintains the transformer turn ratio constant. For the different operation modes of the converters, different switching techniques are applied. Details can be found in [10].

To represent the batteries, the Thevenin equivalent is chosen because it has a simple representation and it is consolidated in the literature for Lead-Acid batteries. This model disregards the state of charge variation of the batteries. However, it is well known that the dynamics related to the charge condition of batteries are slow and do not represent high influence in transient response of the converter.

In the next sections, the analysis of each operation stage of the converter is detailed to obtain its average model for each mode of operation.

*A. Analysis of the converter in charging mode*

During the charging mode, the converter presents four operation stages. In this mode, the DC link converter acts as an inverter and the battery side converter acts as a full bridge rectifier. For the development of the average model, that represents the converter and batteries, the analysis of each individual stage is realized.

**Stage 1: Figure 2-a:** With the switches $S_1$ and $S_4$ in conduction, a positive voltage is applied in the transformer. During this interval of time, the inductor $L_2$ is magnetized and capacitor $C_2$ is charged directly by $V_T$'. Thus $V_{L2} = \frac{V_{DC}}{n} - V_{C2},\ i_{C2} = i_{L2} - \frac{V_{C2} - V_{Bat}}{R_{Bat}}$.

**Stage 2: Figure 2-b:** In the second stage, the switch $S_1$ is blocked applying zero voltage in the transformer. At this moment, the inductor $L_2$ and $C_2$ are discharged. Hence, $V_{L2} = -V_{C2},\ i_{C2} = i_{L2} - \frac{V_{C2} - V_{Bat}}{R_{Bat}}$.

**Stage 3: Figure 2-c:** The switches $S_2$ and $S_3$ are in conduction while $S_1$ and $S_4$ are blocked. The transformer voltage becomes negative while on the low voltage side of the transformer voltage is rectified by the converter and charges the filters $L_2$ and $C_2$ again. Therefore, the analysis performed for stage 1 is valid again.

**Stage 4: Figure 2-d:** Finally, $S_3$ is blocked in order to re-apply a zero voltage on the transformer. The equivalent circuit that results is similar to that presented in stage 2.

If D is the duty cycle of the converter, the static gain for the charging mode is defined as [10]:

$$\frac{V_{Bat}}{V_{DC}} = \frac{D}{n}. \quad (1)$$

To obtain the average model for the charging mode of the converter, the state variables adopted are $i_{L2}$ as well as $V_{C2}$, while the dynamics of the filter $L_1$ and $C_1$ are disregarded, with $V_{C1}$ being approximated to $V_{DC}$. This consideration simplifies the analysis and the model. In this way, the state space converter model for stages 1 and 3 is defined considering:

$$X_1 = i_{L2} \qquad \dot{X}_1 = \frac{V_{L2}}{L_2} = -\left[\frac{1}{L_2}\right]\cdot X_2 + \left[\frac{1}{L_2}\right]\cdot\frac{V_{DC}}{n}, \quad (2)$$

$$X_2 = V_{C2} \quad \dot{X}_2 = \frac{i_{C2}}{C_2} = \left[\frac{1}{C_2}\right]\cdot X_1 - \left[\frac{1}{C_2\cdot R_B}\right]\cdot X_2 + \left[\frac{1}{C_2\cdot R_B}\right]\cdot V_{Bat}. \quad (3)$$

From equations (2) and (3) the state space model is defined by:

$$\begin{bmatrix}\dot{X}_1\\ \dot{X}_2\end{bmatrix} = \begin{bmatrix}0 & -\frac{1}{L_2}\\ \frac{1}{C_2} & -\frac{1}{C_2\cdot R_B}\end{bmatrix}\cdot\begin{bmatrix}X_1\\ X_2\end{bmatrix} + \begin{bmatrix}\frac{V_{DC}}{n\cdot L_2}\\ \frac{V_{Bat}}{C_2\cdot R_B}\end{bmatrix}\cdot u(t), \quad (4)$$

$$[Y] = [1 \quad 0]\cdot\begin{bmatrix}X_1\\ X_2\end{bmatrix}, \quad (5)$$

where u(t) is the unit step function that represents the energization of the system.

The analysis of stages 2 and 4 provides:

$$X_1 = i_{L2} \qquad \dot{X}_1 = \frac{V_{L2}}{L_2} = -\left[\frac{1}{L_2}\right]\cdot X_2, \quad (6)$$

$$X_2 = V_{C2} \quad \dot{X}_2 = \frac{i_{C2}}{C_2} = \left[\frac{1}{C_2}\right]\cdot X_1 - \left[\frac{1}{C_2\cdot R_B}\right]\cdot X_2 + \left[\frac{1}{C_2\cdot R_B}\right]\cdot V_{Bat}. \quad (7)$$

that leads to

$$\begin{bmatrix}\dot{X}_1\\ \dot{X}_2\end{bmatrix} = \begin{bmatrix}0 & -\frac{1}{L_2}\\ \frac{1}{C_2} & -\frac{1}{C_2\cdot R_B}\end{bmatrix}\cdot\begin{bmatrix}X_1\\ X_2\end{bmatrix} + \begin{bmatrix}0\\ \frac{V_{Bat}}{C_2\cdot R_B}\end{bmatrix}\cdot u(t), \quad (8)$$

$$[Y] = [1 \quad 0]\cdot\begin{bmatrix}X_1\\ X_2\end{bmatrix}. \quad (9)$$

To obtain the average state model [14], consider that stages 1 and 3 are represented in the form of (10) and stages 2 and 4 by (11). The matrices $\mathbf{A}_1$, $\mathbf{B}_1$ and $\mathbf{C}_1$ occur for a time proportion to D while matrices $\mathbf{A}_2$, $\mathbf{B}_2$ e $\mathbf{C}_2$ are valid for a time proportional to 1–D.

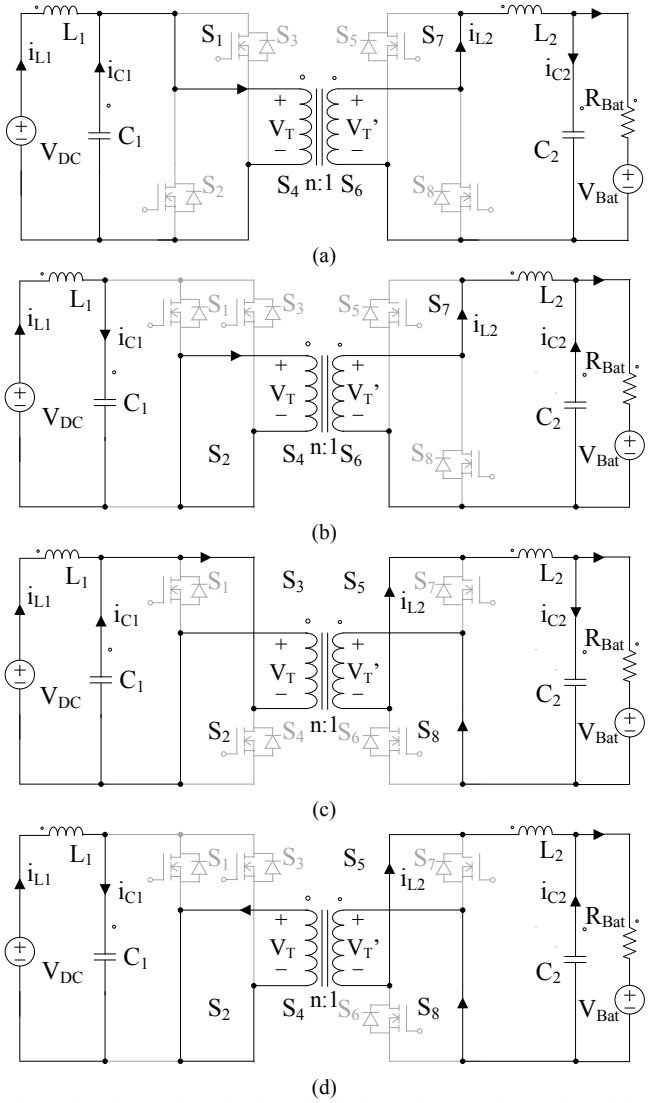


Fig.2. Charging mode equivalent circuits for each stage of operation of the converter.

$$\begin{cases} \dot{\mathbf{X}}_1 = \mathbf{A}_1 \cdot \mathbf{X} + \mathbf{B}_1 \cdot u(t) \\ \mathbf{Y}_1 = \mathbf{C}_1 \cdot \mathbf{X} \end{cases}, \tag{10}$$

$$\begin{cases} \dot{\mathbf{X}}_2 = \mathbf{A}_2 \cdot \mathbf{X} + \mathbf{B}_2 \cdot u(t) \\ \mathbf{Y}_2 = \mathbf{C}_2 \cdot \mathbf{X} \end{cases}, \tag{11}$$

The averaged state space model is given by:

$$\begin{cases} \dot{\mathbf{X}} = \mathbf{A} \cdot \mathbf{X} + \mathbf{B} \cdot u(t) \\ \mathbf{Y} = \mathbf{C} \cdot \mathbf{X} \end{cases} \tag{12}$$

where matrices **A**, **B** e **C** are given by:

$$\mathbf{A} = \mathbf{A}_1 \cdot D + \mathbf{A}_2 \cdot (1-D), \tag{13}$$

$$\mathbf{B} = \mathbf{B}_1 \cdot D + \mathbf{B}_2 \cdot (1-D), \tag{14}$$

$$\mathbf{C} = \mathbf{C}_1 \cdot D + \mathbf{C}_2 \cdot (1-D). \tag{15}$$

The model obtained is called the large signal averaged state space model. It represents the behavior of the converter as a whole and provides the mean value of the transient response. However, since the $V_{DC}$ and $V_{BAT}$ voltages do not depend directly on converter duty cycle, it is necessary to perform the small-signal analysis that is presented in section III.

*B. Analysis of converter in discharging mode*

To define the system model during the discharging mode, each stage of operation of the converter is analyzed again. Considering that the converter is responsible to regulate the DC link, a load, represented by $R_O$ is connected to the system. In this case the battery is considered an ideal voltage source. The analysis of the converter starts in the positive half cycle again, considering the operation in steady state.

**Stage 1: Figure 3-a:** Initially, the switches $S_7$ and $S_6$ are in conduction and a positive voltage is applied to the transformer. During this time, the direct influence of the battery voltage on the circuit charges the capacitor $C_1$ while $L_2$ is demagnetized. The equations involved in this stage are: $V_{L2} = V_{Bat} - \frac{V_{Cl}}{n}$, $i_{C1} = \frac{i_{L2}}{n} - i_{L1}$, $V_{L1} = V_{Cl} - i_{L1} \cdot R_O$.

**Stage 2: Figure 3-b:** To magnetize the inductor $L_2$ again, the switch $S_2$ on the DC link side is in conduction. Thus, the transformer voltage is zero. The energy from the battery is accumulated in inductor $L_2$, while the capacitor $C_1$ is discharged to the output. At this moment $V_{L2} = V_{Bat}$, $i_{C1} = -i_{L1}$ and $V_{L1}=V_{C1}-i_{L1}\cdot R_O$.

**Stage 3: Figure 3-c:** The negative half cycle has two similar stages. When switches $S_5$ and $S_8$ are in conduction, it is applied a negative voltage to the transformer. Initially, capacitor $C_1$ is charged, while $L_2$ is demagnetized, similarly to stage 1.

**Stage 4: Figure 3-c:** Finally, the semiconductor $S_4$ is in conduction magnetizing $L_2$ again while the capacitor $C_1$ discharges, similarly to stage 2.

In discharging mode of the battery bank, the static gain of converter is [10]:

$$\frac{V_{DC}}{V_{Bat}} = \frac{n}{1-D}. \tag{16}$$

During the discharge of the batteries, considering possible failures on DC link, the dynamic response of filter formed by $L_1$ and $C_1$ is included in the average model. In this case, the state variables are: $i_{L1}$, $V_{C1}$ and, $i_{L2}$.

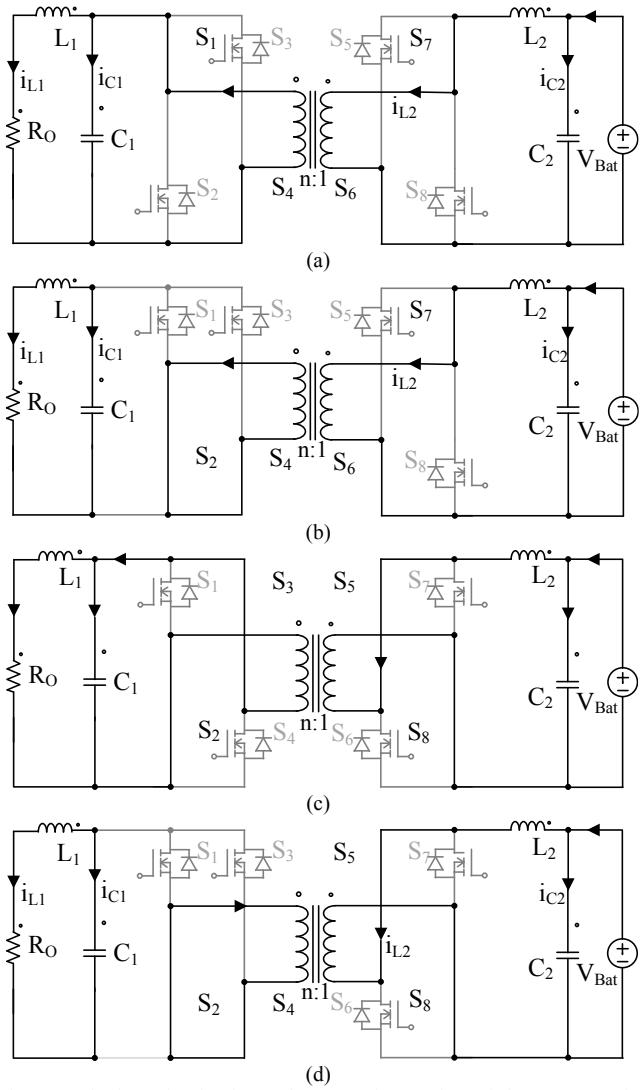


Fig.3. Equivalent circuits for each stage of operation of the converter in battery discharging mode.

From the analysis of the equivalent circuit of the first and third stages, the following equations are obtained:

$$X_1 = i_{L2} \qquad \dot{X}_1 = \frac{V_{L1}}{L_1} = -\left[\frac{R_O}{L_1}\right]\cdot X_1 + \left[\frac{1}{L_1}\right]\cdot X_2, \tag{17}$$

$$X_2 = V_{C1} \qquad \dot{X}_2 = \frac{i_{C1}}{C_1} = -\left[\frac{1}{C_1}\right]\cdot X_1 + \left[\frac{1}{n\cdot C_1}\right]\cdot X_3, \tag{18}$$

$$X_3 = i_{L2} \qquad \dot{X}_3 = \frac{V_{L2}}{L_2} = -\left[\frac{1}{L_2\cdot n}\right]\cdot X_2 + \left[\frac{1}{L_2}\right]\cdot V_{Bat}, \tag{19}$$

Hence, the state space model are:

$$\begin{bmatrix}\dot{X}_1\\ \dot{X}_2\\ \dot{X}_3\end{bmatrix} = \begin{bmatrix}-\frac{R_O}{L_1} & \frac{1}{L_1} & 0\\ -\frac{1}{C_1} & 0 & \frac{1}{n\cdot C_1}\\ 0 & -\frac{1}{n\cdot L_2} & 0\end{bmatrix}\cdot\begin{bmatrix}X_1\\ X_2\\ X_3\end{bmatrix} + \begin{bmatrix}0\\ 0\\ \frac{V_{Bat}}{L_2}\end{bmatrix}\cdot u(t) \tag{20}$$

$$[Y] = [0 \quad 1 \quad 0]\cdot\begin{bmatrix}X_1\\ X_2\\ X_3\end{bmatrix}. \tag{21}$$

Considering the second and fourth operating stages, the following equations are valid:

$$X_1 = i_{L2} \qquad \dot{X}_1 = \frac{V_{L1}}{L_1} = -\left[\frac{R_O}{L_1}\right]\cdot X_1 + \left[\frac{1}{L_1}\right]\cdot X_2, \tag{22}$$

$$X_2 = V_{C1} \qquad \dot{X}_2 = \frac{i_{C1}}{C_1} = -\left[\frac{1}{C_1}\right]\cdot X_1, \tag{23}$$

$$X_3 = i_{L2} \qquad \dot{X}_3 = \frac{V_{L2}}{L_2} = \left[\frac{1}{L_2}\right]\cdot V_{Bat}. \tag{24}$$

These equations provide the state space model that is given by:

$$\begin{bmatrix}\dot{X}_1\\ \dot{X}_2\\ \dot{X}_3\end{bmatrix} = \begin{bmatrix}-\frac{R_O}{L_1} & \frac{1}{L_1} & 0\\ -\frac{1}{C_1} & 0 & \frac{1}{n\cdot C_1}\\ 0 & -\frac{1}{n\cdot L_2} & 0\end{bmatrix}\cdot\begin{bmatrix}X_1\\ X_2\\ X_3\end{bmatrix} + \begin{bmatrix}0\\ 0\\ \frac{V_{Bat}}{L_2}\end{bmatrix}\cdot u(t) \tag{25}$$

$$[Y] = [0 \quad 1 \quad 0]\cdot\begin{bmatrix}X_1\\ X_2\\ X_3\end{bmatrix}. \tag{26}$$

Again, from the models obtained for each stage of operation, the average model in state space are obtained, according to the same methodology previously adopted for the charging mode.

## III. SMALL-SIGNAL MODELS AND EXPERIMENTAL RESULTS

Both models developed in the previous section represent the large signal dynamics of the converter. Since the average model in state space depends on the inputs $V_{DC}$ and $V_{BAT}$, which does not depend directly on the control action, the obtained models are not interesting for the design of controllers. Therefore, it is necessary to perform an adequate mathematical manipulation in the average model to represent it as a function of the duty cycle D.

The analysis showed in [14] results in the so-called small-signal model. This model is obtained around a point of operation and has as input variable a magnitude associated with the manipulation of converter duty cycle and is therefore suitable for control purposes.

The small signal averaged model for any converter is defined by the analysis of perturbations on the state variables of the system. From this principle, the mathematical analysis presented by [14] results in the model given by:

$$\dot{\hat{\mathbf{x}}} = \mathbf{A}\cdot\hat{\mathbf{x}} + \mathbf{B}_s\cdot \mathrm{d}, \qquad \mathbf{y} = \mathbf{C}\cdot\hat{\mathbf{x}}, \tag{27}$$

where $\mathbf{B_s}$ is equal to

$$\mathbf{B}_s = (\mathbf{A}_1 - \mathbf{A}_2)\cdot(-\mathbf{A}^{-1}\cdot\mathbf{B}) + (\mathbf{B}_1 - \mathbf{B}_2). \tag{28}$$

From equation (27) it is observed that the model of small-signal depends on input d, which represents variations of converter duty cycle over a point of operation and is, therefore, suitable for the control.

To validate the obtained models, experimental results were obtained in open loop using a prototype built for this purpose. The converter parameters are summarized in Table I.

TABLE I
DETAILS OF CONVERTER COMPONENTS

| Components | Parameters |
|---|---|
| Transformer | Transformer ratio (2:1) |
| Inductor $L_1$ | 0.5 mH |
| Capacitor $C_1$ | 470 nF / 250 V |
| Indutor $L_2$ | 1,50 mH |
| Capacitor $C_2$ | 47 nF / 150 V |
| Load ($R_O$) | 265 Ω |
| Battery Bank | Nominal Voltage: 60 V ( 5xGP12170 )<br>Capacity: 17 Ah<br>Internal resistance ($R_{Bat}$): 0,1 Ω<br>Charge current: 0,1 C ( 1,7 A) |
| Switch Frequency | 50 kHz. |
| DC link Voltage | 230 V. |

The converter transient response is obtained using a Tektronix DPO4034 oscilloscope. The measured response is compared with simulations carried out using PSIM software. The experimental data were saved in vectors and treated using Matlab software.

### *A. Simulation and experimental results of converter operating in charging mode*

The transient response of converter during the charging process was obtained using the step response method. According to the manufacturer's instructions, the batteries must be charged with currents between 0.85 A and 1.70 A, therefore, the converter duty cycle was defined using equation (1) to result in adequate current values.

Initially, to verify the validity of the large signal model, two situations were performed using PSIM: a) Considering the battery bank totally discharged when the voltage is equal to 54 V; b) Battery bank fully charged, when the batteries must have a maximum voltage equal to 70 V.

The large signal model for the charging mode of the converter is defined by equations (4), (5), (8) and (9), replaced in the model presented by (12).

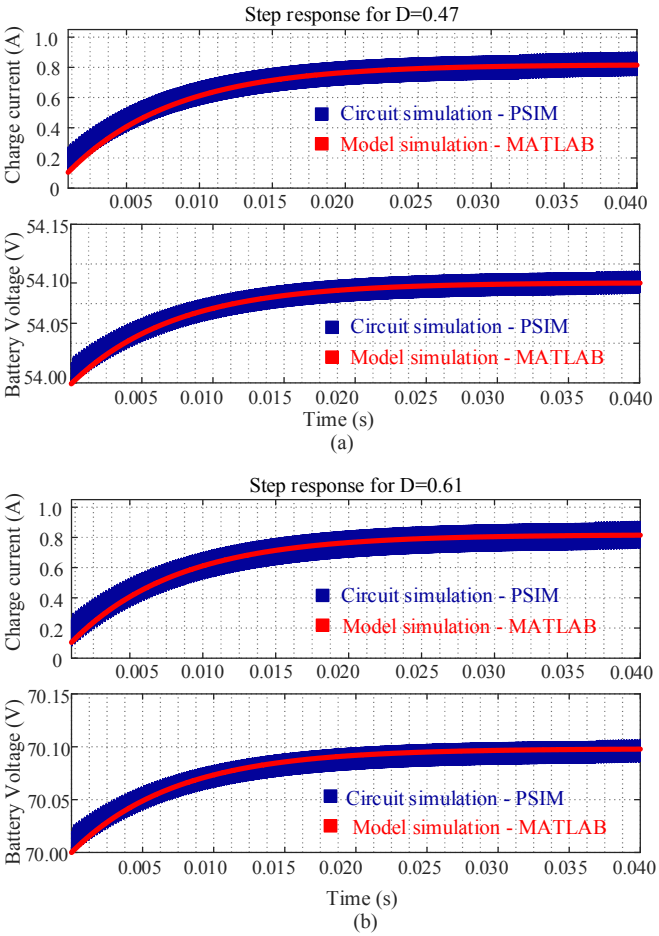


Fig.4. Response of the large signal averaged model for the charging mode: a) considering the batteries with a voltage equal to 54 V; b) considering the batteries with a voltage of 70 V.

The result is shown in Figure 4, where the coherence of the large signal models for different points of operation is verified. From this result it can be verified that the averaged model obtained in the previous section describes adequately large signal variations.

To validate de small signal model, a discharged battery bank with 53 V was considered. The converter was simulated with a duty cycle equal to 0.4617, which results in a charging current equal to 0.90 A. A perturbation of 0.001 is applied on the converter duty cycle that leads the battery current during the charge to its nominal value (1.7 A). Similar experimental test was performed in the laboratory to compare the converter response with the simulations. The results are presented in Figure 5.

Based on the result presented in Figure 5, it is observed that the small-signal model provides a similar response to that obtained in the circuit simulation and to the experimental setup result. It must be noticed that even considering simplifications during the modeling, the small signal model provides adequate transient response.

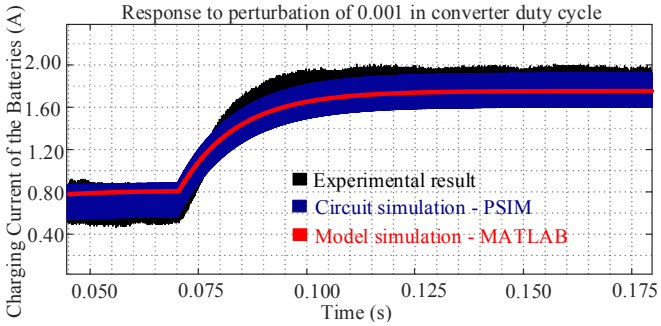


Fig.5. Comparison between the response of the small-signal model with the experimental results and simulation of the circuit for a disturbance on the duty cycle of the converter.

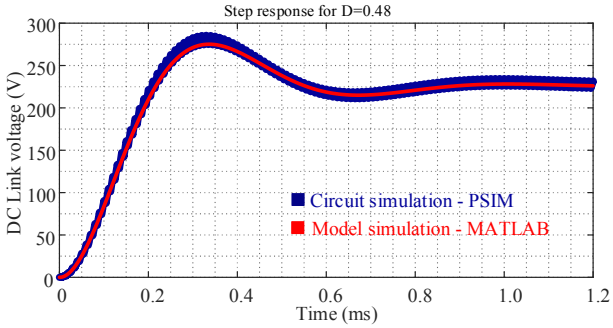


Fig.6. Comparison between the simulations of the circuit and the large signal averaged model of the converter operating in the discharging mode.

Considering the parameters presented in Table I, using the matrices that describe the state space model of the converter for the charge mode for the batteries charge mode and the equation (27), that defines the small-signal model, the transfer function (29) can be obtained. The transfer function is useful to design the controller of the converter for the charging mode.

$$G_A(s) = \frac{i_B(s)}{d(s)} = \frac{1.44 \cdot 10^5 s + 2.5 \cdot 10^{13}}{s^2 + 1.7 \cdot 10^8 s + 1.3 \cdot 10^{10}}. \quad (29)$$

It can be seen from equation (29) that through the small-signal approach, the converter model can be expressed as a ratio of the load current and the variation of the duty cycle.

*B. Simulation and experimental results of the converter operating in discharging mode*

During the discharging mode of operation, the inverter must regulate the voltage of the DC bus. For this situation, the converter duty cycle is set to result in values close to the nominal DC link voltage, 230 V.

To verify the large-signal model, the step response of the obtained model was simulated using Matlab and it was compared with the results obtained by the simulation of the circuit, performed using PSIM software. The simulations were performed considering the battery bank fully charged, with 60 V nominal voltage. Therefore, it operates at nominal voltage. In this case, the nominal converter duty cycle is 0.48.

The comparison between the model response and the simulated circuit is presented in Figure 6. It can be seen that the averaged model of the circuit describes the behavior of the circuit considering large signal variations. To validate the small signal model, initially the converter was simulated with a duty cycle equal to 0.40. For this condition, the output voltage is equal to 200 V. After a time of 1.50 ms a perturbation of 0.08 is applied on the converter duty cycle, which takes the DC link voltage to the value of 230 V. Similarly, the converter was tested in laboratory with the same operation point. The result is shown in Figure 7, which compares the response of the simulations with the experimental result of the converter.

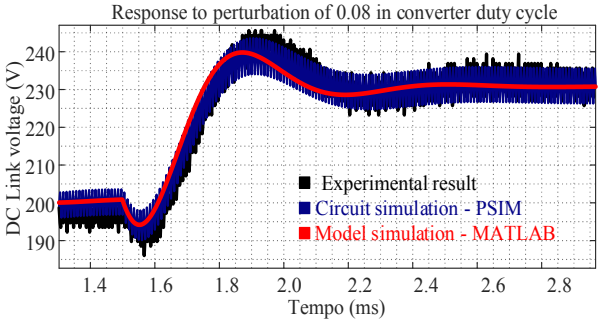


Fig.7. Comparison between the averaged small-signal model response with the experimental results and simulation of the circuit for the converter operating in the discharging mode.

Comparing the responses of the simulated circuit, the small-signal model and the experimental result of the converter, it is observed that both simulated systems present a transient response similar to the experimental result. Therefore, the result presented by Figure 7 corroborates the mathematical model obtained.

Based on the small-signal model, the transfer function representation is obtained (30). It relates the output voltage of the converter with the perturbations of the duty cycle.

$$G_B(s) = \frac{V_{DC}(s)}{d(s)} = \frac{-2.29 \cdot 10^6 s^2 - 1.05 \cdot 10^{12} s + 2.18 \cdot 10^{16}}{s^3 + 4.802 \cdot 10^8 s^2 + 4.08 \cdot 10^9 s + 7.86 \cdot 10^{13}} \quad (30)$$

Since the transfer function depends on the duty cycle, the small-signal model is suitable for the controller design, which must keep the DC link voltage constant during the discharging of the batteries.

Another point to be mentioned is the inclusion of the Thevenin model of the batteries in the converter small-signal models. Using this approach, it was possible to include the influence of the batteries in the converter model in its different modes of operation. In both cases, it was not considered dynamics related to variations in the state of charge of the batteries. However, the experimental results shown that these variations do not affect, significantly, the transient response of the system.

## IV. CONCLUSIONS

This paper presented the modeling of an isolated bidirectional battery charger. Two models were proposed: one for the converter operating in the charging mode and

another model for the converter operating in the discharging mode. Both models include the presence of battery bank that are disregarded in previous works available in literature. All the models are presented to be easily used for the design of controllers. Simulation and experimental results were presented to validate the models.

## ACKNOWLEDGMENTS

This study was financed in part by the Coordenação de Aperfeiçoamento de Pessoal de Nível Superior - Brasil (CAPES) - Finance Code 001. The authors would like to thank to the Research and Development project PD 2866-0468/2017, granted by the Brazilian Electricity Regulatory Agency (ANEEL) and Companhia Paranaense de Energia (COPEL). The authors also thank to FINEP, SETI, CNPq, Fundação Araucária and UTFPR for additional funding.

## REFERENCES

[1] P. M. Curtis, "UPS Systems: Applications and Maintenance with an Overview of Green Technologies" Wiley-IEEE Pres, 1ª Ed. p. 223-264, 2011.

[2] M. H. Rashid, "Power Electronics Handbook: devices, circuits and applications handbook" 3ª Ed. Elsevier – Oxford, 2011.

[3] T. Tao, J. L. Duarte, M. A. M. Hendrix, "Line-Interactive UPS Using a Fuel Cell as the Primary Source" IEEE Transactions on Industrial Electronics, Vol. 55, No. 8, 2008.

[4] C. Jabayabalu, K. Sarbham, "Single Stage High- Gain Boost Converter With Battery Commutation In Solar Power Applications" International Journal of Science, Engineering and Technology Research (IJSETR), Vol. 4, No. 5, 2015.

[5] X. Hu, C. Gong, "A High Gain Input-Parallel Output-Series DC/DC Converter with Dual Coupled-Inductors" in IEEE Transactions on Power Electronics Vol. 30, No. 3, 2015.

[6] L. Schuch, C. Rech, H. Leães, H. A. Grudling, H. Pinheiro, J. R. Pinheiro, "Analysis and Design of a New High-Efficiency Bidirectional Integrated ZVT PWM Converter for DC-Bus and Battery-Bank Interface" IEEE Transactions On Industry Applications, Vol. 42, No. 5, p. 1321-1333, 2006.

[7] N. M. L. Tan, T. Abe, H. Akagi, "Design and Performance of a Bidirectional Isolated DC-DC Converter for a Battery Energy Storage System", IEEE Transactions on Power Electronics, Vol. 27, no. 3, p. 1237-1248, 2012.

[8] H. Akagi, N. M. L. Tan, S. Kinouchi, Y. Miyazaki, M. Koyama, "Power-Loss Breakdown of a 750-V 100-kW 20-kHz Bidirectional Isolated DC–DC Converter Using SiC-MOSFET/SBD Dual Modules" IEEE Transactions On Industry Applications, Vol. 51, No. 1, p. 420-428, 2015.

[9] H. Wen, W. Xiao, B. Su, "Nonactive Power Loss Minimization in a Bidirectional Isolated DC–DC Converter for Distributed Power Systems" IEEE Transactions on Industrial Electronics, Vol. 61, No. 12, 2014.

[10] E. L. Carvalho, E. Carati, G.; J. P. Costa, C. M. O. Stein, R. Cardoso, "Design and Analysis of a Bidirectional Battery Charger". 8th International Symposium on Power Electronics for Distributed Generation Systems - PEDG 2017, 2017, Florianópolis - SC. Proceedings of 8th International Symposium on Power Electronics for Distributed Generation Systems - PEDG 2017.

[11] B. Zhao, Q. Song, W. Liu, Y. Su, "Overview of Dual-Active-Bridge Isolated Bidirectional DC–DC Converter for High-Frequency-Link Power-Conversion System" IEEE Transactions on Power Electronics, Vol. 29, No. 8, 2014.

[12] C. Zhao S.D. Round J.W. Kolar, "Full-order averaging modelling of zero-voltage-switching phase-shift bidirectional DC–DC converters" IET Power Electronics, Vol. 3, Iss. 3, 2010.

[13] H. Qin, J. W. Kimball, "Generalized Average Modeling of Dual Active Bridge DC–DC Converter" IEEE Transactions on Power Electronics, Vol. 27, No. 4, 2012.

[14] R. W. Erikson, D. Maksimovic, "Fundamental of Power Electronics" Kluwer Academic/Plenum Publishers, 2ª ed.- Boulder, Colorado. 2001.